Impact of Geometric Design on Thermal Efficiency of Heat Sinks

Derraz Hanaa[1], Bencherif Atika[2] , Medjeded Afafe[3] , Bouzit Mohamed[4]

[1,2,3,4]*Laboratory of Maritime Sciences and Engineering LSIM Faculty of Mechanical Engineering, University of Science and Technology of Oran, Mohamed Boudiaf, El Mnaouar, B.P.1505, 31000, Oran, Algeria.*

E-mail: hanaa.derraz@univ-usto.dz , Atika.bencherif@univ-usto.dz , afafe.medjeded@univ-usto.dz , mohamed.bouzit@univ-usto.dz .

Abstract: The study focuses on the in-depth analysis of flow and heat transfer phenomena within a heat sink. This research relies on a numerical methodology using the finite element method and primarily aims to assess the impact of using a nanofluid to enhance heat dissipation of the heat sink. Specifically, this investigation explores various influential parameters. Initially, the Hartmann number is systematically varied from 0 to 50 to examine the influence of magnetic fields on the heat sink's performance. Additionally, kinematics is examined by modifying the Reynolds number over a range from 5 to 60. Moreover, the purpose of the study is to determine the effect of heat sink geometry on heat transfer. The results from this comprehensive numerical approach are presented in the form of velocity and Temperature contours, graphically illustrating flow patterns, as well as Nusselt plots, quantifying heat transfer. These visual and numerical data provide substantial contributions to understanding heat sink cooling mechanisms, particularly concerning the application of nanofluids under various operational conditions.

Keywords: Electronic heat sink, non-Newtonian fluid, heat transfer, cooling capacity, finite elements.

1. INTRODUCTION

Despite substantial advancements in recent years, the electronics industry and semiconductor technology continue to encounter significant challenges related to the cooling of high-performance, high-heat flux products. Conventional cooling methods and standard refrigerants do not meet the cooling requirements of electronic chips that produce a considerable amount of heat. As a result, high-efficiency electronic devices require innovative approaches and coolants with exceptional thermal properties to dissipate the generated heat and achieve the expected performance and reliability (Sharma et al ., 2013).

Research has shown that mini-channel cooling systems using liquids as coolants are among the most effective solutions for modern electronics cooling (Arani et al.,2017). Additionally, suspensions containing solid nanoparticles, known as nanofluids, display markedly superior thermal properties compared to traditional coolants (Hosseini et al., 2019). Numerous researchers have reviewed studies on nanofluids across various fields, including friction factor and convective heat transfer (Sundar et al ., 2013), the use of nanofluids in boiling heat transfer (Wu et al.,2013), particle migration in nanofluids (Bahiraei et al.,2016), mass transfer in nanofluids (Ashrafmansouri et al .,2014), and entropy generation in nanofluids (Mahian et al .,2013). These studies generally reveal excellent properties of nanofluids in heat transfer systems (Imani-Mofrad et al .,2018). Furthermore, limited evaluations of nanofluids in liquid blocks also suggest that this new class of suspensions performs better in cooling electronics than conventional fluids. Indeed, innovative cooling techniques such as mini-channel systems, combined with these novel fluids, can significantly enhance heat dissipation efficiency and meet the cooling demands of high-temperature electronic equipment. Consequently, nanofluid-based liquid blocks represent a promising option for the next generation of electronic cooling devices.

In this study, we review the research conducted on the application of nanofluids in electronics cooling. Various aspects such as liquid block geometry, nanoparticle material, numerical approach, and the second law of thermodynamics are examined. Additionally, the gaps and challenges in this field are identified and discussed, and several directions for future research are suggested. It is important to note that different researchers have used various parameters to evaluate the thermal performance of heat sinks. The thermal resistance of heat sinks, the average temperature of the heated surface, and the maximum temperature of the heated surface, the convective heat transfer coefficient, the Nusselt number, and temperature uniformity have been the most commonly used characteristics to compare the thermal performance of different heat sinks or different nanofluids.

2. MATHEMATICAL MODEL

The geometry of the problem under study consists of a rectangular duct with dimensions $L \times H$, as illustrated in Figure 1. Within this duct, identical hot cylindrical electronic components with a diameter d are introduced, as depicted in Figures 1 through 3. A nanofluid flows through this duct in a laminar regime to cool these electronic components.

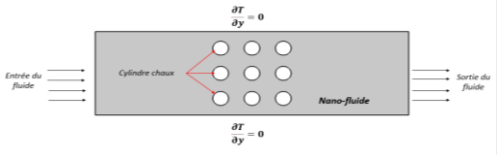

Figure .1. Internal boundaries of the domain

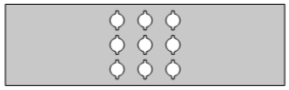

Figure .2. Studied geometry (2)

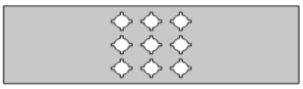

Figure .3. Studied geometry (3)

The characteristics of the nanofluid, including those of the base fluid and nanoparticles, are mentioned in the following table1

Table :1 Physical properties of the base fluid and nanoparticles

Physical Properties	Density [kg/m^3]	Dynamic Viscosity [Pa.s]	Thermal Conductivity [W/(m.K)]	Specific Heat [J/(kg.)]	Electrical Conductivity [S/m]	Thermal Expansion [1/K]
Water	997.1	0.001	0.613	4179	0.050	21.0×10^{-5}
Al_2O_3	3970	-	40.00	765.0	1×10^{-10}	0.85×10^{-5}

Continuity equation

$$\frac{\partial u}{\partial x}+\frac{\partial v}{\partial y}=0 \quad (1)$$

Momentum equation

$$\rho_{nf}\left(\frac{\partial u}{\partial t}+u\frac{\partial u}{\partial x}+v\frac{\partial u}{\partial y}\right)=-\frac{\partial p}{\partial x}+\mu_{nf}\left(\frac{\partial^2 u}{\partial x^2}+\frac{\partial^2 v}{\partial y^2}\right) \quad (2)$$

$$\rho_{nf}\left(\frac{\partial v}{\partial t}+u\frac{\partial v}{\partial x}+v\frac{\partial v}{\partial y}\right)=-\frac{\partial p}{\partial y}+\mu_{nf}\left(\frac{\partial^2 v}{\partial x^2}+\frac{\partial^2 v}{\partial y^2}\right)+\rho_{nf}g\beta_{nf}(T-T_c)-\sigma_{nf}B^2v \quad (3)$$

Energy equation

$$\rho_{nf}cp_{nf}\left(\frac{\partial T}{\partial t}+u\frac{\partial T}{\partial x}+v\frac{\partial T}{\partial y}\right)=k_{nf}\left(\frac{\partial^2 T}{\partial x^2}+\frac{\partial^2 T}{\partial y^2}\right) \quad (4)$$

Boundary conditions

At the inlet

$$v=0\,,u=0\,,T=T_c$$

At the outlet

$$\frac{\partial u}{\partial x}=\frac{\partial v}{\partial x}=\frac{\partial T}{\partial x}=0\ et\ p=0$$

On the channel walls

$$\frac{\partial T}{\partial x}=\frac{\partial T}{\partial y}=0\ et\ u=v=0$$

At the cylinders

$$T=T_h$$

$$\overline{Nu}=\frac{\bar{h}D_h}{k}$$

3. SOLUTION METHODOLOGY

The numerical simulation plays a pivotal role in understanding the complex dynamics of fluid-flexible fin interactions. To accurately solve the governing equations and boundary conditions, a Galerkin weighted residual method, specifically the finite element method, is employed on a moving grid system. This allows for the consideration of fluid-structure interactions, which are crucial in this scenario. An Arbitrary Lagrangian-Eulerian (ALE) approach is utilized to account for the fluid-flexible fin interaction, providing a robust framework for analyzing such coupled problems.

3.1. Computational grid and mesh independent study

The computational domain is carefully discretized into non-uniform triangular elements. This non-uniform meshing technique captures the intricate flow behavior near the fin's surface, ensuring accurate representations of the boundary layer effects. To streamline the nonlinear terms within the momentum equations, a Newton iteration algorithm is implemented, facilitating faster and more stable convergence. The mesh refinement near the walls, consisting of 92,491 elements, strikes a balance between computational accuracy and efficiency, delivering precise results without excessive computation times and data sizes. The convergence criterion is stringent, requiring a relative error of less than 10^{-6} for each variable. This stringent criterion. ensures that the simulated results are highly accurate and reliable, providing a robust foundation for further analysis and insights into the complex thermal dynamics within the system. The careful consideration of meshing techniques, element types, and convergence criteria showcases the thoroughness of the numerical approach, contributing to the overall reliability of the study's findings

Table: 2 Mesh independent study

Elements	7651	13479	42430	92491	157737
Nu	4.231692	4.401572	4.427415	4.428125	4.428085

3.2. Numerical validation

In order to ensure the reliability of our numerical results, we compared them with previous works. By placing ourselves in their simulation conditions, we highlighted the variation of the average Nusselt number as a function of the Hartmann number, see Figur 4. Comparing our results with those of Hussain and Ahmed [3], it clearly appears that there is a very satisfactory agreement and coherence, which validates our numerical results.

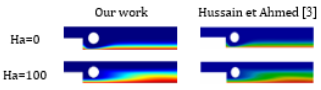

Figure.4. Comparison of thermal profiles with the results of Hussain et al., (2019)

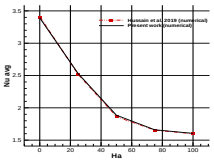

Figure .5. Comparison of the average Nusselt number with Hussain et al., (2019)

4. RESULTS AND DISCUSSION

The presented results will focus on the influence of geometric design, Reynolds and Hartmann parameters, as well as nanoparticle concentration on the flow configuration, characterized by temperature and velocity contours. Additionally, the impact on heat transfer will be studied by analyzing the variations in Nusselt number curves.
Text of the subsection.

Figure 6 illustrates the velocity contours of three different heat sink geometries for various Reynolds numbers at Ha = 25, G = 0, and φ = 0.05. An increase in the Reynolds number indicates an increase in both fluid velocity and turbulence.

For the first geometry, the increase in Reynolds number corresponds to a rise in velocity and fluid turbulence, resulting in a slight increase in the intensity of the streamlines. However, in geometries 2 and 3, the effect becomes more pronounced, with an increase in Reynolds number leading to the formation of small vortices between the heat sink fins and at the exit of the third column. These vortices grow larger as the Reynolds number increases. It is important to note that the vortices formed at the exit of the third column are significantly larger than those formed between the fins, highlighting the enhanced impact of increasing the Reynolds number on vortex formation

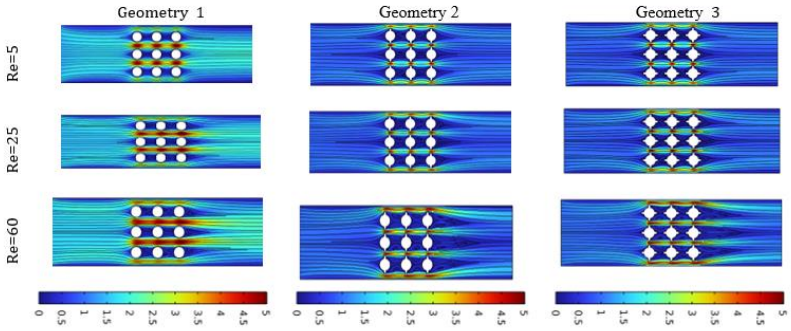

Figure.6. Velocity contours for different Reynolds number values at Ha = 25, G = 0, and φ = 5%.

Figure 7 presents the temperature contours for different Reynolds numbers (Re), with Ha = 25, G = 0, and φ = 5%.

The isothermal contours reveal the influence of increasing Reynolds numbers on the thermal field. For low Re values, there is a concentration of temperature variation around the fins and downstream of the conduit, where the isotherms occupy a significant portion of the channel. This results in a moderate decrease in temperature in these regions. As the Reynolds number increases (Re = 25, 50, 60), a reduction in the thermal boundary layer thickness near the fins (heat source) is observed. This can be attributed to improved heat dissipation to the exterior and reduced thermal congestion, indicating enhanced convective heat transfer. Additionally, geometries 1 and 3 demonstrate more efficient heat dissipation compared to geometry 2.

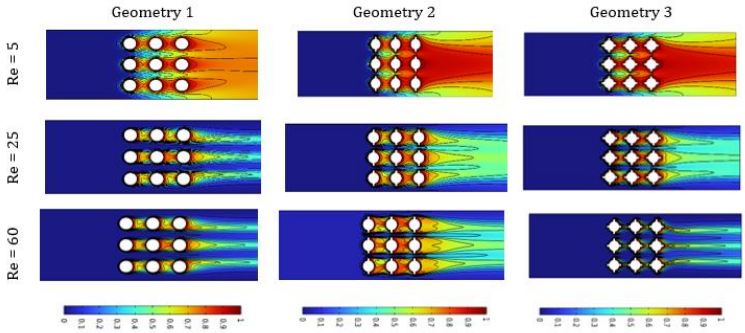

Figure.7. Temperature contours for different Reynolds number values at Ha = 25, G = 0, and φ = 5%.

Figures 8 and 9 depict velocity and temperature contours for three types of heat sinks at different Hartmann numbers (Ha) with Re = 60, G = 0, and φ = 5%.

Upon observing the velocity and temperature contours, slight changes were noted for the first geometry, which featured smooth cylindrical fins. However, an interesting phenomenon was observed for the second and third geometries. At Ha = 0,

the formation of a large vortex near the third column was evident. This large vortex significantly influences the flow patterns. Nevertheless, as the Hartmann number (Ha) increased, it was observed that this vortex decreased in size.

This observation suggests that the application of a magnetic field, represented by the Ha parameter, has a notable effect on flow behavior in the second and third geometries. Specifically, increasing Ha appears to reduce the magnitude of the formed vortex, which could have significant implications for heat transfer and overall thermal dissipation performance of the heat sink.

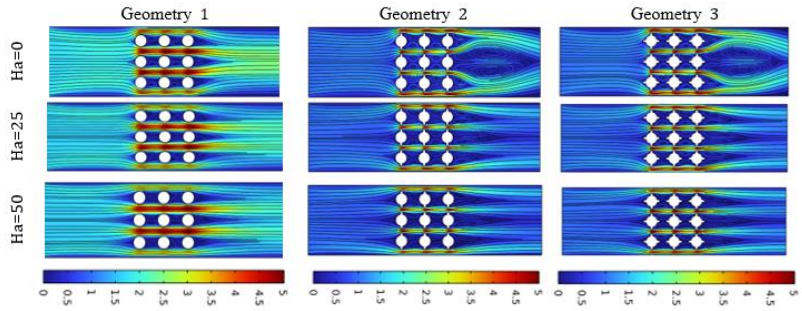

Figure.8. Velocity contours for different Hartmann number values at Re = 60, and φ = 0.05

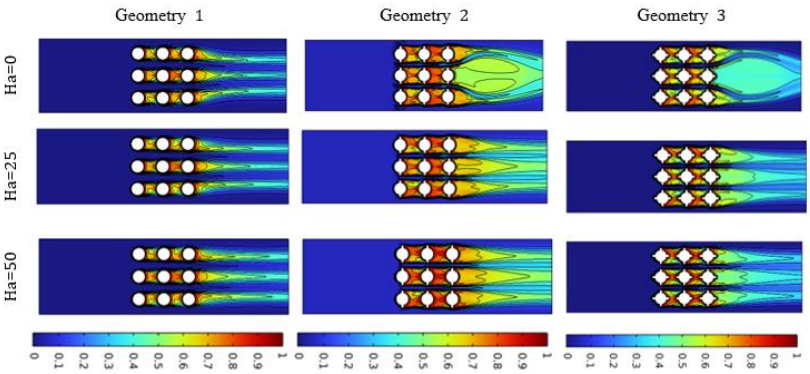

Figure .9. Temperature contours for different Hartmann number values at Re = 60, and φ = 5%

Figure 9 presents the Nusselt number graph as function of Hartmann number (Ha) for three Reynolds numbers (5, 25, 60) across three different heat sink geometries. Significant observations were made during the analysis of these results.

For the first geometry, a notable discrepancy among the five curves is observed. It is noted that at Re = 60, the Nusselt number exhibits the highest value compared to all other Reynolds numbers studied, indicating a significant enhancement in heat transfer for this specific configuration. In contrast, for the second and third geometries, although differences among the curves are also observed, they are less pronounced. The curve corresponding to Re = 60 for the first geometry shows a higher Nusselt number than that of the second and third geometries.

These findings underscore the importance of heat sink geometry in heat transfer efficiency. They indicate that different geometries may exhibit varying thermal performance under specific conditions. Thus, in the context of this study, the first geometry proves to be more effective in terms of heat transfer compared to the second and third geometries when Re equals 60.

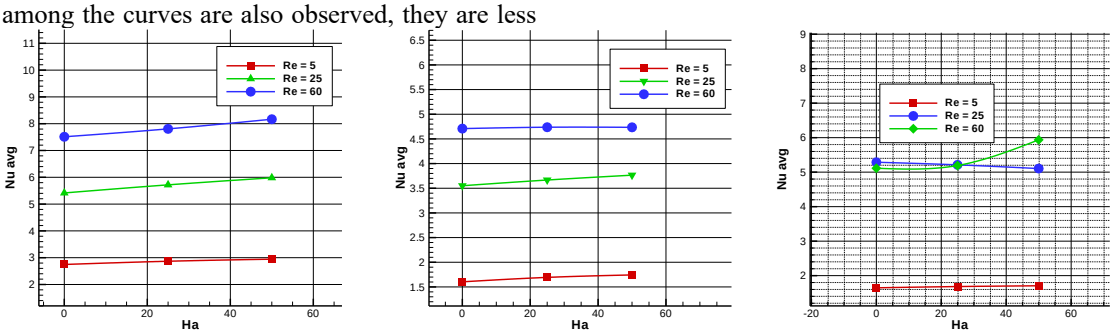

(Geometry 1) (Geometry 2) (Geometry 3)

Figure.10. Nusselt graph as a function of Ha

Figure 11 presents the Nusselt number graph as a function of Reynolds number (Re) for three Hartmann numbers (Ha = 0, 25, 50) across three different heat sink geometries.
Regarding the first geometry, the disparity among the curves for different Ha values indicates a significant variation in the thermal performance of the heat sink. Specifically, for Ha = 50, the curve exhibits the maximum Nusselt number, suggesting a substantial enhancement in heat transfer compared to other Ha values.Conversely, for the second geometry, the curves are nearly overlapping, indicating a limited influence of Ha on the heat sink's thermal performance. This can be attributed to the specific configuration of the second geometry, which may stabilize heat transfer, thereby reducing the impact of Ha variation. These observations underscore the importance of heat sink geometry in heat transfer efficiency and demonstrate that different geometries may respond differently to Ha variations

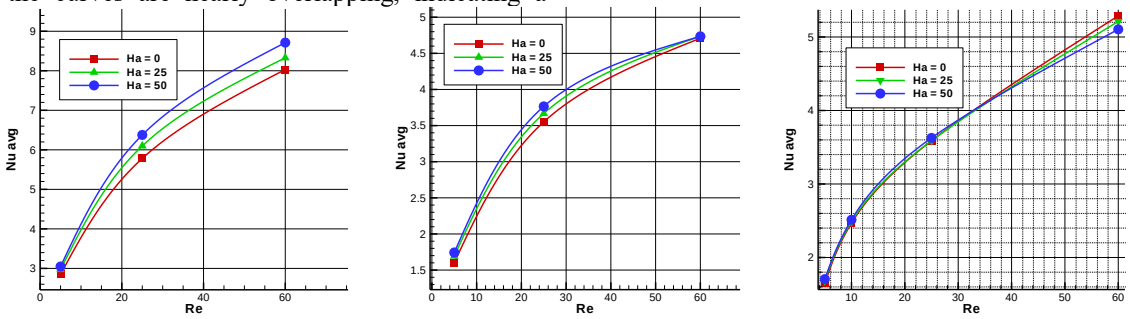

(Geometry 1) (Geometry 2) (Geometry 3)

Figure .11. Nusselt graph as a function of Re

5. CONCLUSION

A heat sink is a heat-conducting metal device designed to absorb and disperse heat from a high-temperature object. Typically, heat sinks are installed inside fans to help dissipate heat and keep the component at the correct temperature for it to work properly. They are attached to the top of the component.

As the Reynolds number increases, the intensity of the current lines increases slightly. Increasing the Reynolds number causes inertial forces to dominate, intensifying the recirculation zones. The Reynolds number has a considerable effect on the increase in the Nusselt number.

The variation in the Hartmann number makes a difference to the flow of the nanofluid. The cooling of hot springs is observed as a function of the Hartmann number, with a moderate difference.

Generally speaking, the values of the mean Nusselt number for the nanofluid are higher than those for the pure fluid.

This numerical study explored several aspects of heat transfer and flow phenomena in different systems. The results obtained demonstrated the importance of taking into account parameters such as Reynolds number, Hartmann number and the geometry of the heat sink in order to optimise thermal performance. In particular, the geometry with smooth fins gave better results than the other geometries.

REFERENCES

Arani, A. A. A., Akbari, O. A., Safaei, M. R., Marzban, A., Alrashed, A. A., Ahmadi, G. R., & Nguyen, T. K. (2017). Heat transfer improvement of water/single-wall carbon nanotubes (SWCNT) nanofluid in a novel design of a truncated double-layered microchannel heat sink. International Journal of Heat and Mass Transfer, 113, 780-795.

Ashrafmansouri, S. S., & Esfahany, M. N. (2014). Mass transfer in nanofluids: A review. International Journal of Thermal Sciences, 82, 84-99.

Bahiraei, M. (2016). Particle migration in nanofluids: a critical review. International Journal of Thermal Sciences, 109, 90-113.

Hosseini, S. M., Safaei, M. R., Goodarzi, M., Alrashed, A. A., & Nguyen, T. K. (2019). New temperature, interfacial shell dependent dimensionless model for thermal conductivity of nanofluids. International Journal of Heat and Mass Transfer, 114, 207-210.

Imani-Mofrad, P., Heris, S. Z., & Shanbedi, M. (2018). Experimental investigation of the effect of different nanofluids on the thermal performance of a wet cooling tower using a new method for equalization of ambient conditions. Energy conversion and management, 158, 23-35.

Mahian, O., Kianifar, A., Kleinstreuer, C., Moh'd A, A. N., Pop, I., Sahin, A. Z., & Wongwises, S. (2013). A review of entropy generation in nanofluid flow. International Journal of Heat and Mass Transfer, 65, 514-532.

Sharma, C. S., Tiwari, M. K., Michel, B., & Poulikakos, D. (2013). Thermofluidics and energetics of a manifold microchannel heat sink for electronics with recovered hot water as working fluid. International Journal of Heat and Mass Transfer, 58(1-2), 135-151.

Sundar, L. S., & Singh, M. K. (2013). Convective heat transfer and friction factor correlations of nanofluid in a tube and with inserts: a review. Renewable and Sustainable Energy Reviews, 20, 23-35.

Wu, J. M., & Zhao, J. (2013). A review of nanofluid heat transfer and critical heat flux enhancement—research gap to engineering application. Progress in Nuclear Energy, 66, 13-24.